Biotechnology Journal

DOI 10.1002/biot.201000394

Biotechnol. J. 2011, 6, 156–164

Research Article

Deep wells integrated with microfluidic valves for stable docking and storage of cells

Yun-Ho Jang[1,2], Cheong Hoon Kwon[1,2], Sang Bok Kim[1,2], Šeila Selimović[1,2], Woo Young Sim[1,2], Hojae Bae[1,2], Ali Khademhosseini[1,2,3]

[1] Center for Biomedical Engineering, Department of Medicine, Brigham and Women's Hospital, Harvard Medical School, Cambridge, MA, USA
[2] Harvard-MIT Division of Health Sciences and Technology, Massachusetts Institute of Technology, Cambridge, MA, USA
[3] Wyss Institute for Biologically Inspired Engineering, Harvard University, Boston, MA, USA

In this paper, we describe a microfluidic mechanism that combines microfluidic valves and deep wells for cell localization and storage. Cells are first introduced into the device via externally controlled flow. Activating on-chip valves was used to interrupt the flow and to sediment the cells floating above the wells. Thus, valves could be used to localize the cells in the desired locations. We quantified the effect of valves in the cell storage process by comparing the total number of cells stored with and without valve activation. We hypothesized that in deep wells external flows generate low shear stress regions that enable stable, long-term docking of cells. To assess this hypothesis we conducted numerical calculations to understand the influence of well depth on the forces acting on cells. We verified those predictions experimentally by comparing the fraction of stored cells as a function of the well depth and input flow rate upon activation of the valves. As expected, upon reintroduction of the flow the cells in the deep wells were not moved whereas those in shallow wells were washed away. Taken together, our paper demonstrates that deep wells and valves can be combined to enable a broad range of cell studies.

Received 15 November 2010
Revised 3 January 2011
Accepted 5 January 2011

Supporting information available online

Keywords: Cell docking · Deep wells · Microfluidics · Microfluidic valves

1 Introduction

In the past few years there has been a steady effort in the bioengineering community to develop new tools for cell storage [1], culture [2–4], and analysis [5, 6], specifically using microscale technologies [7], for example microfluidics [8]. Advantages of microfluidic devices such as small reagent volumes and short reaction times are well-known, but they are especially important in biological applications, e.g., in high-throughput cell screening operations. One of the challenges of conducting cell studies in microfluidic devices is achieving uniform cell seeding inside microfluidic chambers [9, 10]. The other issue is long-term cell storage or culture inside microscale chambers [11–13].

There have been several approaches to immobilize cells within microfluidics [14], especially for high-throughput applications by encapsulating cells in droplets [15, 16], trapping cells in microsieves [17, 18], well-plating [19] and by using patch-clamp arrays [20]. While effective for cell trapping, these methods have limitations for conducting high-throughput cell assays. Encapsulating cells in droplets is useful for building and analyzing thousands of samples simultaneously, but it is difficult to culture cells for a long time due to the limited volume of nutrients in the droplets, as well as space available to hold daughter cells. Cell trapping in microsieves and well-plates can be used to conduct single cell analysis, the cells, however, are

Correspondence: Dr. Ali Khademhosseini, Center for Biomedical Engineering, Department of Medicine, Brigham Woman's Hospital, Harward Medical Scholl Cambridge, MA 02139, USA
E-mail: alik@rics.bwh.harvard.edu
Fax: +1-617-768-8477

continuously exposed to external fluidics. This can possibly lead to flow-induced effects on cells, such as mechanotransduction. Patch-clamp is useful for analyzing the mechanical and electrical properties of cells, but this device causes mechanical stress on cells. Micron sized well arrays were used to capture single cells and to transfer the cells onto a culture plate for stem cell environmental studies [21], or the captured cells were cultured inside well arrays [22]. These approaches are useful for capturing single cells in a controlled manner; however, in both cases the transferred cells still experience shear stress from the external flow. Additionally, expansion of the method for high throughput analysis is difficult since all captured cells are exposed to the same conditions, and incorporation of microfluidic channels and valves is not easy after cell manipulation. Work conducted by Hung et al. [12, 23] shows a promising design for perfusion cultures, but there is a limitation to expand to high-throughput analysis since it is hard to incorporate microfluidic valves for compartmentalization of each chamber. Recently Han *et al*. [24] have reported microwell based single oocyte trapping, which is simpler for such large cells (~100 μm) than for most other. Finally cell docking inside wells was analyzed by examining flow recirculation regions [25], but the device was not coupled with microfluidic valves, restricting cell docking applications.

This paper aims to address these challenges by describing a poly(dimethylsiloxane) (PDMS) microfluidic chip that allows cells to be anchored and held undisturbed in deep storage wells, without being affected by the surrounding flow. The proposed device is a three-layer PDMS device, with passive flow channels and storage wells built into the bottom layer, and active control channels or valves incorporated into the upper layer (Fig. 1A). The two thick layers are separated by the third layer, a thin PDMS membrane. In one variation of this design 15 wells are placed along a single straight channel. Surrounding each well are two peristaltic valves, [26] placed on top of each flow channel segment leading to the well, such that they can allow or inhibit flow through the channel and into the chamber. When the valves are open (or inactive), fluids and suspensions can flow through the channel to the wells. The incoming particles such as cells slow down as they pass above the wells, but are not immediately trapped. It is only when all valves are closed (or active) that further flow is inhibited and cells floating above the wells can sediment into the wells. Within a few hours after sedimentation, cells can adhere to the PDMS surface [27]. A key feature of this well design relative to its predecessors is its large depth. Once the cells are trapped on the bottom of a deep well, the shear stress acting on them cannot displace them. This is true for sufficiently deep wells even when valves are open. Thus, deep wells in concert with integrated valves acts as a reliable cell trapping and long-term storage mechanism.

2 Materials and methods

A PDMS device was fabricated consisting of a single, straight, 100 μm wide flow channel in which flow can be controlled by on-off peristaltic valves as shown in Fig. 1B. Every 800 μm along the channel a storage well is placed in the middle of the channel, with a total of 15 wells. Figure 1C shows a cross-sectional view of the fabricated device consisting of control channel, a thin membrane, and a deep well. A single control line leads to all valves placed between wells, and each valve extends 200 μm beyond the flow channel, allowing for a low closing pressure and reliable on-off operation. The protocol for fabricating the silicon master molds and the PDMS device can be found in the Supporting information (Table S1).

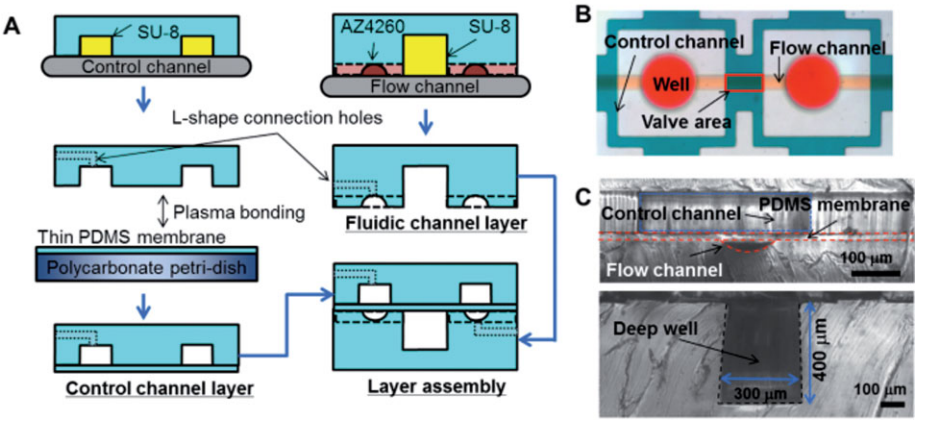

Figure 1. Fabrication process and device structure. (A) Thick PDMS layers (~4 mm) are cast from two silicon molds and a thin PDMS membrane (15 μm) is spin-coated on a poly-carbonate Petri dish. L-shape connection gates are punched before layer assembly. The detailed process is described in Supporting Information. (B) Top view of the fabricated device shows deep wells and flow channels (red) and control channels (dark green). (C) Cross-sectional view of the flow channel and a well.

2.1 Simulation of flow in wells

To evaluate the hydrodynamic characteristics and the cell behavior in the proposed microfluidic structure, fluid dynamic simulations were performed using the COMSOL software. The flow field in the microfluidic structure is determined by solving the steady-state Navier–Stokes equation

$$\rho(\mathbf{v}\cdot\nabla)\mathbf{v} = -\nabla p + \mu\nabla^2\mathbf{v}, \quad (1)$$

where $\mathbf{v}$ is the velocity vector, p the pressure, ρ and μ are density and dynamic viscosity of the fluid, respectively. The microfluidic structure is modeled by using a 2-D geometry; for the cell culture medium we assume ρ = 1000 kg/m^3 and μ = 0.001 Pa s [28]. To predict the cell behavior, a disk-shaped model cell (radius r = 5 μm) was placed on the bottom of the well and the shear stress acting on the cell boundary was calculated. The shear stress is obtained from the flow field simulation and the flow-induced force from the line integration [29].

$$\mathbf{F} = F_x\hat{\mathbf{x}} + F_y\hat{\mathbf{y}} = \int_{\partial\Omega}\tau_s dl, \quad (2)$$

where F_x and F_y are x- and y-directional force, respectively. The shear stress (τ_s) was integrated along the disk boundary ($\partial\Omega$) to find the total force acting on the cell cultured on 2-D surface.

In this computation we imposed a non-slip condition on the wall and cell boundary for three different inlet velocities (0.0028 m/s–20 μL/h, 0.014 m/s–100 μL/h, and 0.070 m/s–500 μL/h) and three well depths (150, 250, and 400 μm). A constant velocity at the inlet and a constant pressure was assumed with no viscous stress at the outlet. The flow field was computed to evaluate the flow-induced force on the cell located at 15 different positions on the bottom of the well with a 20 μm pitch.

2.2 Cell culture

Unless indicated otherwise, reagents were obtained from Sigma–Aldrich (St. Louis, MO, USA). MCF7 breast cancer cells were cultured in high glucose-DMEM (Gibco, USA) supplemented with 10% fetal bovine serum (FBS) and penicillin–streptomycin (Gibco, USA) and kept at 95% O_2/5% CO_2 humidified 37°C incubator. Cells were harvested using 0.05% trypsin-EDTA (Gibco, USA) and resuspended in culture medium [30].

2.3 Effect of valve activation on cell trapping

We conducted two different sets of experiments to test the effect of valve activation on cell trapping. In the first set, we observed the cell docking behavior without activating valves by conducting nine different experiments, in which we varied the well depth and the flow rate, similar to our simulations (see above). We chose a relatively low cell concentration of 10^5 cells/mL in order to prevent cell aggregation and clogging of the channel. The cell suspension was loaded into the device with a 1 mL plastic syringe (Becton-Dickinson) driven by a syringe pump (Harvard PhD 2000) for 6 min. We then stopped the flow by turning off the syringe pump and recorded images of all wells using an upright microscope (Nikon TE2000-U, 4× achromat objective). We counted the number of cells stored in each well and computed the average number of cells per well, and the SD for all well depths, and for all flow rates.

In the second set of nine experiments we observed the cell docking behavior in the presence of activated control valves. In this set of experiments the control channels or control valves were filled with water and connected to a nitrogen tank with a pressure controller, as is commonly done when operating on-off peristaltic valves [31]. We first introduced cells into the flow channel for 2 min at the selected flow rates and then closed the valves fully by applying a pressure of 60 kPa to the control lines for 3 min. We then opened the valves and reintroduced the flow for an additional 4 min. Finally, we stopped the syringe pump without activating the valves again and counted the number of stored cells per well.

2.4 Effect of well depth on cell trapping in presence of activated valves

Nine devices and cell suspensions for testing the three different well depths at three different flow rates were prepared like described in the section above, except with a higher concentration of cells (10^6 cells/mL). We introduced the flow of cells for 2 min, then closed the valves and stopped the syringe pump. At this point cells began to sink to the bottom of the storage wells. Three minutes later we imaged all wells. We then turned on again the syringe pump using the same flow rate as before and also opened the valves. After 1 min and at constant flow we imaged the wells a second time in order to compare the number of cells that were stored prior to and after valve activation.

2.5 Cell viability test

To assess the viability of the cells in our experiments, we used three devices with 400 μm deep wells to measure the number of live and dead cells

after 0, 12, and 24 h inside microfluidic chambers. The devices used in these experiment contained a grid of 16 × 16 orthogonally placed channels with wells placed at all intersections. As in our simpler devices, all channel branches could be controlled by activating valves.

Cells were injected manually from the four corners of the well array and stored as described above. Then the device was immersed in a 6 well plate filled with medium and kept for 0, 12, and 24 h in a 95% O_2/5% CO_2 humidified 37°C incubator. Afterward, cells were stained for 15 min with the Live/Dead Viability/Cytotoxicity Kit (Invitrogen, USA), Calcein AM for live cells and Ethidium homodimer (EthD-1) for dead cells. The excitation/emission wavelengths for Calcein and Ethidium homodimer are 494/517 nm and 528/617 nm, respectively. Then the device was washed with PBS for 10 min. We recorded fluorescence images of the cells using a 4× objective, with dead cells appearing red and live cells appearing green for more than 90 wells in each device. We counted the number of red and green fluorescent cells in each well, normalized each number against the total number of cells per well and calculated the average fraction of live cells inside well array to obtain cell viability values.

2.6 Statistical analysis

Data were expressed as average values with the SD as error bars. Differences between groups were analyzed using the two-tailed Student *t*-test with *p*-values less than 0.05 considered significant and represented by a single star in the graphs.

3 Results and discussion

3.1 Simulation of flow in wells

We performed a computational fluid dynamic calculation to evaluate the flow field and flow-induced forces on cells inside wells. Figure 2 shows flow streamlines and flow-induced force distribution for different well depths and cell locations. In Fig. 2A, the streamlines of the flow field were obtained at a flow rate of 500 μL/h with a cell located in the middle of the well bottom. For well depths of 150 and 250 μm, the flow profiles were similar, as shown in Figs. 2A and 2B. A small microcirculation region was observed in the corners of the well as described previously [32]; the flow direction near the cell was the same as for the mainstream flow for shallow wells. For the 400 μm deep well, however, a large microcirculation region formed near the bottom of the well. As a consequence, the flow direction near the cell was opposite to the mainstream flow direction.

In addition to the flow field we also calculated the flow induced forces on a cell. We assumed that the cell is stationary and located in the various positions of the bottom of the well. In observation of the flow-induced force distribution in 150 and 250 μm deep wells, x-directional flow-induced force had a maximum in the middle of the bottom surface and was nearly zero in the corner regions. Our interpretation is that a cell could move along the positive x-direction and remain locked in the corner when the flow-induced force overcomes the cell adhesion force which is in agreement with previous cell alignment study using microgrooves [28]. Additionally, the cell experiences a downward force near the incoming channel region and a lift force near the exit channel region. The direction of the x- and y-components of the flow-induced force on cells in 400 μm deep wells is opposite to that in shallow wells due to the formation of the large microcirculation region in the deep well.

The magnitude of the flow-induced force increased with the inlet velocity and inlet flow rate. For all wells, the y-component of the shear force was approximately one order of magnitude smaller than the x-directional force component. Moreover, the flow-induced force decreased sharply with y-position of the cell inside the well, as it sank to the bottom. For the 400 μm deep well, the flow-induced force was roughly two orders of magnitude smaller than in the 150 μm deep well. Cells can be trapped in wells when the well is deep or the flow rate is low, however, the deep well is more practical as it allows the cell docking and storage at a wider range of flow rates.

3.2 Effect of valve activation on cell trapping

The cell localization and docking procedure due to activating valves is depicted in Fig. 3A. The flow channel under valves used in this device has an inverted round shape which closes the flow channel with a low pressure as simulated in Fig. S1 in Supporting information. We used 60 kPa to control valves based on the preliminary experiment (Fig. S1). Closing the valves stopped the flow, allowing the cells floating in the flow path and above the wells to settle to the bottom surface of a well. The cells remaining in the main flow channel were flushed out after the flow was reestablished. Figure 3B shows the effect of the well depth and flow rate on the average number of stored cells per well. When valves were open, few cells could be stored inside the wells, as most cells had a forward velocity that was larger than the speed with which they sank to the bottom of a well. When the valves were activated

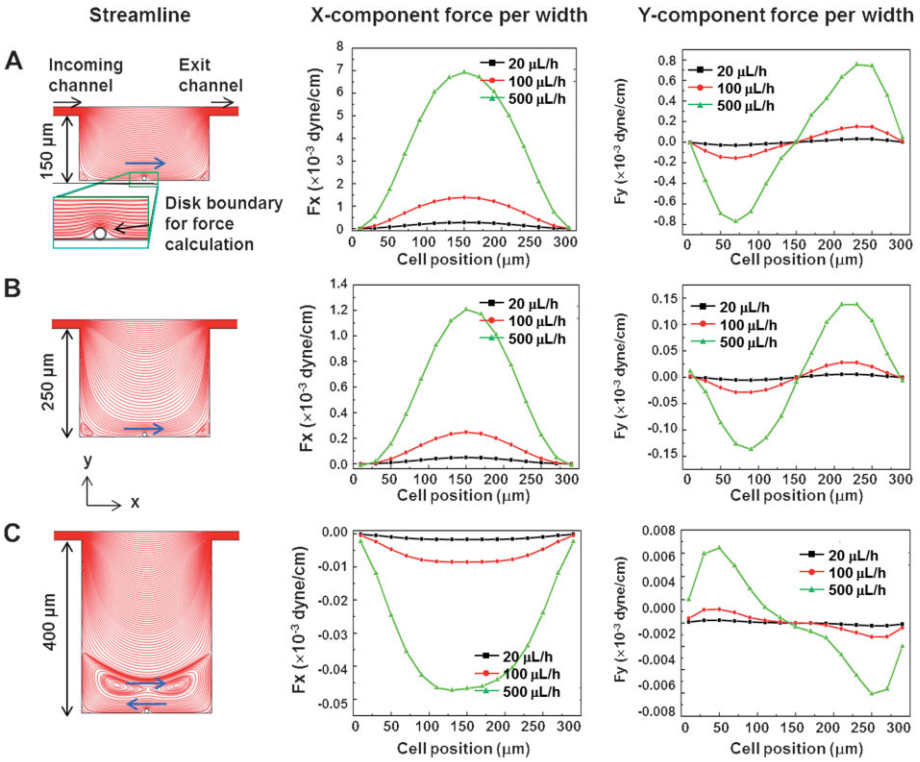

Figure 2. Flow field simulation and flow-induced force distribution for different depths of the well (A) 150 µm, (B) 250 µm, and (C) 400 µm. Far left column shows flow streamlines when a single cell is located in the middle of the well bottom with a flow rate of 500 µL/h. The microcirculation region expands in deep wells to reverse the flow direction on the bottom of the well, which aids the docking and storing of cells. X- and Y-force components show that the force acting on cells decreases rapidly with increasing depth.

(closed), the average number of captured cells was significantly higher and statistically different from the number of cells when the valves were open. We reduced the concentration of cells in order to avoid clogging of the channel and applied the flow for a short time, thus a number of wells remained empty, causing the large SD. This experiment implies that the external flow control alone without valve activation is not sufficient for stable cell docking. This is because cells follow flow streamlines and flow was required to cease to allow cells to fall into the well bottom.

3.3 Effect of well depth on cell trapping in presence of activated valves

Figure 4 shows time sequence images of three wells varying in depth with captured MCF7 cells. In panels A, C, and E the valve was closed at $t = 0$ after an initial flow rate of 100 µL/h; in panels B, D, F the valve was opened after 3 min and a 100 µL/h flow rate was reestablished for an additional 0.6 s. The falling time of MCF7 cells was roughly 1 min for the 400 µm deep wells. There was no other mechanism at play other than sedimentation that drives the

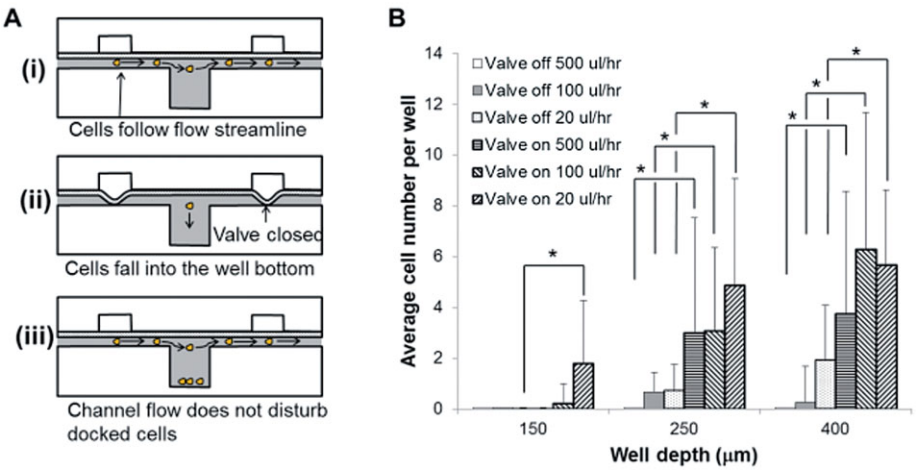

Figure 3. (A) Cell docking and storage within microwells by controlling valves. (B) Average number of cells stored in wells at different flow rates (20, 100, 500 µL/h) and well depths (150, 250, 400 µm), with and without valve activation. * shows a statistically significant difference in variance ($p < 0.05$).

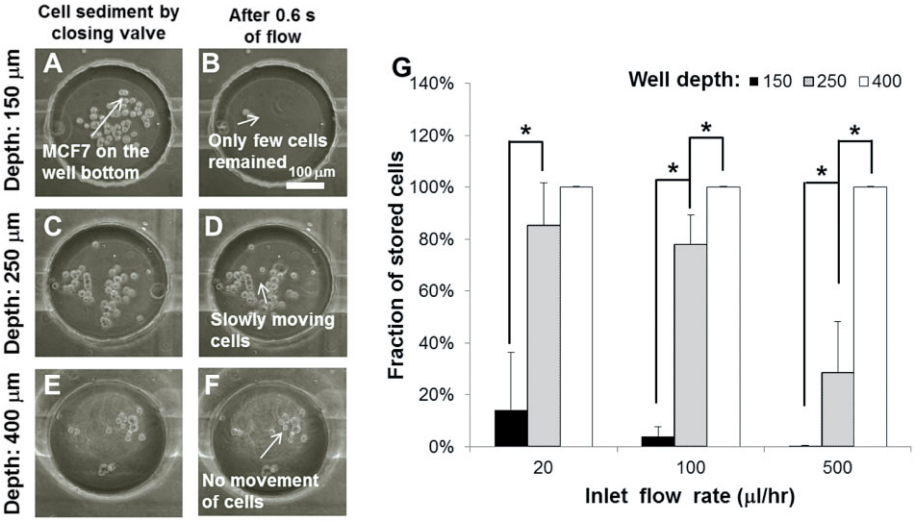

Figure 4. Cell docking and storage experiments with phase contrast images in time sequence at an inlet flow rate of 100 μL/h. Three different depths of wells were compared; 150 (A–B), 250 (C–D), 400 μm (E–F). The bottom surface of the wells was in focus in all images. (G) The statistical data for fraction of stored cells after opening valves and allowing flows. * shows a statistically significant difference in variance ($p < 0.05$).

cells toward the bottom well surface by a gravity force.

As shown in Fig. 4A, almost all settled cells were washed out by the reestablished flow, and only 3.8% of initially settled cells were retained in the wells. The fraction of stored cells was slightly higher (14.2%) at 20 μL/h, but zero at a high flow rate of 500 μL/h (Fig. 4G). Increasing the well depth to 250 μm resulted in improved cell retention (up to 80% at low flow rates), however, the fraction of retained cells was still highly dependent on the applied flow rate and dropped significantly at 500 μL/h. Statistical analysis showed that the deeper wells increased the fraction of cells for all flow rates except the lowest flow rate (20 μL/h) since the shear force was not sufficiently strong to move cells in case of low flow rates. Moreover, some cells that remained captured at these conditions shifted their position on the well surface, indicating that it may not be possible to store them for a long period of time. We achieved the best cell retention results at a well depth of 400 μm. Here, all of the initially settled cells remained captured without changes in their position at 100 μL/h and with only slight movement at 500 μL/h. We note that in this experiment we were interested in the fraction of cells that remained stored after reintroduction of the flow, so we only gathered information about the cell number from five wells in each device.

3.4 Cell viability test

To demonstrate the applicability of deep wells in concert with on-off valves to cell studies we performed a series of cell viability tests as a function of cell storage time (Fig. 5). We used 400 μm deep wells to store cells effectively. The only modification to the standard experimental procedure was the immersion of the device in PBS for 24 h in order to enhance cell viability on the PDMS surface. The three devices used for 0, 12, and 24 h culture periods on average contained between 45 and 70 cells per well when we manually (without a syringe pump) injected the cell suspension, while using on-off valves. The cells sank to the well bottom within 1 min. Figures 5A, C, E shows that cells formed a monolayer on the well bottom just after sedimentation, as well as cell attachment after 12 h; therefore, we can count live and dead cells using microscope images to assess viability. The random positioning of cells also indicates that the cells were not affected by the channel flow after sedimentation: had the cells strongly experienced the channel flow they would have moved to or aligned toward the low shear stress region [28, 32]. The cell viability after seeding (0 h) was 97.4%. Twelve hours after seeding many cells were observed to attach and spread on the PDMS surface as shown in Figs. 5C, D. At this time the viability was 91.1%, and reduced to 88.2% after another 12 h as summarized in Fig. 5G. Previous studies describe the enhanced effect of coating PDMS with biocompatible materials such as fibronectin on cell spreading and viability [11, 33]. Additionally, dynamic culture through media perfusion inside a microfluidic device is reported to increase the viability from 75 to 85% after 13 days [34]. These results imply that higher cell viability can be obtained in a long-term culture by coating the surface of the storage chamber with biocompatible materials and flowing culture media to supply cells adequately with nutrients. We note that we did not measure the flow of oxygen into and changes in oxygen concentration inside wells, as those experiments are beyond the scope of

Biotechnol. J. 2011, 6, 156–164

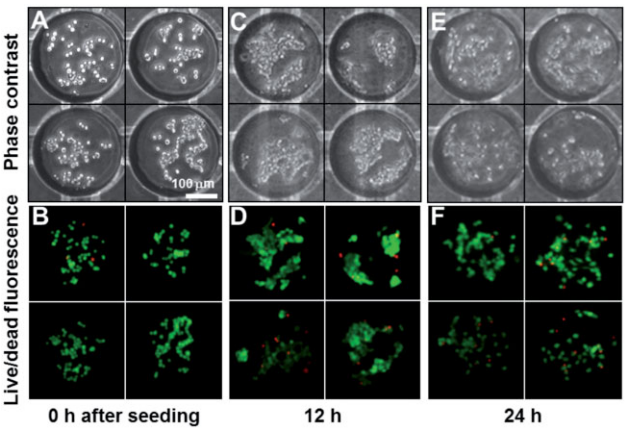

Figure 5. MCF7 cell viability in a microfluidic device containing an array of 16 × 16 wells (depth: 400 μm) for up to 24 h. (A–F) Phase images and fluorescent images with calcein AM (green, live)/ ethidium homodimer (red, dead), (G) cell viability at 0, 12, and 24 h after seeding cells in the microfluidic device.

this study, but they will be addressed in future research.

This study provides a cell docking and storage mechanism by combining deep wells with microfluidic valves, and the effect of deep wells is interpreted by computational analysis on flow induced forces. We showed that valve activation effectively stopped the flow and increased the number of docked cells, and that the cells stored in shallow wells (150 μm deep and 300 μm wide) were easily washed out while cells stored in deep wells (400 μm deep and 300 μm wide) were not disturbed by an externally applied flow rate up to 500 μL/h (0.070 m/s). Our computational analysis suggests that a microcirculation region forms even in shallow wells, but the shear force in shallow wells is large enough to displace them as we demonstrated with experiments.

We performed numerical simulations to obtain flow-induced forces on a cell, and further to evaluate the effect of well depths on cell docking. The calculated flow induced force acting on cells stored at the bottom of a 400 μm deep well was two orders of magnitude smaller than the force in a 150 μm deep well. We confirmed this result experimentally by comparing the fractions of stored cells in either case. The numerical calculation provided a comparison of forces acting on cells in wells of different depths, however it has limitations: First, the simulation model was 2D for fast evaluation of forces, but it is difficult to estimate accurate forces acting on cells located inside 3D environments. Second, it is difficult to anticipate whether cells move or not under a certain flow rate since the information about stiction or frictional forces of docked cells is limited and should be measured.

Previous studies showed that cells were docked on the low shear stress regions in the bottom of wells and grooves [25, 28, 32]. The cells were attached to the surface or were trapped in microcirculation regions. While these approaches are useful to load cells inside microfluidic devices without further integration of active valves, they have some limitations: First, the inlet flow rate should be small to avoid flushing cells out from the wells and grooves. This limits the range of applied flow rates after cell docking. Second, cells aligned easily with trench edges when they were trapped in microcirculation regions. This alignment can be beneficial when we need to place cells at selected locations, although cells forming a monolayer are preferable for optical analysis. These limitations can be overcome by using deep wells integrated with valves. The valves stop the flow completely; therefore cells can sink to the well bottom and form a monolayer (Fig. 5). Once the cells are docked in a deep well, the flow induced force is too small to move the cells, allowing a large range of flow rates after cell storage. This low shear force is advantageous for cells when there is continuous flow in the channel. Cells docked in a deep well experience a smaller shear force so that side effects of the flow, such as mechanotransduction, are less likely.

One of possible limitations of this mechanism is an effective delivery of nutrients and retrieval of metabolites from cells located on the bottom of wells since diffusion time increases as the depth of well increases. The diffusion time of oxygen in a 400 μm deep well filled with water is calculated to be less than 30 s based on the equation, $t = x^2/(2 \times D)$, where t is the time, x the characteristic distance (400 μm), and D is the diffusion coefficient of oxygen (3×10^{-9} m^2/s [35]). Moreover, PDMS is permeable to air [36] so that environmental oxygen can be supplied through PDMS. Therefore, we can improve material exchange by controlling the valves to stop the flow and to allow material to be diffused fully inside wells or by exposing the PDMS surface to external air to absorb oxygen through PDMS.

A potential advantage of the proposed mechanism is an easy expansion to a large number of wells for high throughput cell analysis. This would entail fabricating a dense and large array of wells, connecting the wells via fluidic channels, docking cells inside deep wells, and controlling the flow with valves. The effect of flow on cells inside fluidic channels can be minimized due to the large depth of wells, but the incoming solutions can nonetheless reach the cells located on the well bottom *via* diffusion when flow is inhibited. Uniform cell loading in each well is still challenging, however, and may require both delicate design strategies to obtain a uniform cell suspension inside the microfluidic chip and the preparation of a homogeneous cell suspension.

4 Concluding remarks

The results of this study lead us to two conclusions: first, activating on-off valves that surround a storage chamber help us localize cells and reduce their forward velocity to zero, allowing them to settle to the bottom of a well. This alone leads to an improved ability to capture cells. Second, the shear stress acting on cells stored in deep wells as opposed to shallow wells is small and a recirculation region at the bottom of the well is formed, helping to retain the stored cells in their chambers. Therefore, the valve activation improved cell docking by stopping flow and allowing cell sedimentation, and the deep well stored cells even under a high flow rate (500 μL/h–0.07 m/s) in a flow channel. The cell viability was monitored to demonstrate the application of the device on cell experiments and to show that nearly 90% of the cells remaining viable after 24 h in culture.

The main advantages of the proposed mechanism is stable cell trapping and possible application to long term storage more than 24 h, as cells cannot leave the wells at moderately fast input flows. The possibility of integrating a perfusion system and inclusion of microfluidic valves can be utilized for many additional purposes, such as directed access to a particular storage chamber. When extended to a large well array, this mechanism could potentially be used for high-throughput cell studies with temporal and spatial flow control, e.g., analyzing the cell response to various factors important in cell function and differentiation.

In summary, we demonstrate the advantages of this device, including pressure efficient valves and stable cell storage wells, which is useful for biological applications. The design and fabrication approach described here can be utilized for high throughput cell analysis, as it allows for reliable long-term cell storage.

This paper was supported by the National Institutes of Health (EB008392; HL092836; EB009196; DE019024), National Science Foundation (DMR0847287), the Institute for Soldier Nanotechnology, the Office of Naval Research, and the US Army Corps of Engineers. Y. H. Jang was partially supported by the National Research Foundation of Korea Grant funded by the Korean Government [NRF-2009-352-D00107]. W. Y. Sim was partially supported by the Korea Research Foundation Grant funded by the Korean Government [KRF-2008-357-D00099].

Y. H. J., W. Y. S., Š. S., and A. K. designed the study. Y. H. J. fabricated the devices. Y. H. J. and C. H. K. conducted experiments, S. B. K. and Y. H. J. conducted computer simulations. Y. H. J. and C. H. K. analyzed the data. All authors wrote and edited the paper.

The authors have declared no conflict of interest.

5 References

[1] Walter, W., Jr., Palma, C., Effect of long-term storage on cell wall neutral sugars and galacturonic acid of two sweetpotato cultivars. *J. Agric. Food Chem.* 1996, *44*, 278–281.

[2] Rosler, E., Fisk, G., Ares, X., Irving, J., *et al.*, Long term culture of human embryonic stem cells in feeder free conditions. *Dev. Dyn.* 2004, *229*, 259–274.

[3] Folkman, J., Haudenschild, C., Zetter, B., Long-term culture of capillary endothelial cells. *Proc. Natl. Acad. Sci. USA.* 1979, *76*, 5217–5221.

[4] Gartner, S., Kaplan, H., Long-term culture of human bone marrow cells. *Proc. Natl. Acad. Sci. USA.* 1980, *77*, 4756–4759.

[5] Zeng, X., Rao, M., Human embryonic stem cells: Long term stability, absence of senescence and a potential cell source for neural replacement. *Neuroscience* 2007, *145*, 1348–1358.

[6] Jaiswal, J., Mattoussi, H., Mauro, J., Simon, S., Long-term multiple color imaging of live cells using quantum dot bioconjugates. *Nat. Biotechnol.* 2002, *21*, 47–51.

[7] Khademhosseini, A., Langer, R., Borenstein, J., Vacanti, J., Microscale technologies for tissue engineering and biology. *Proc. Natl. Acad. Sci. USA.* 2006, *103*, 2480–2487.

[8] Gu, W., Zhu, X., Futai, N., Cho, B., Takayama, S., Computerized microfluidic cell culture using elastomeric channels and Braille displays. *Proc. Natl. Acad. Sci. USA.* 2004, *101*, 15861–15866.

[9] Lee, P., Hung, P., Rao, V., Lee, L., Nanoliter scale microbioreactor array for quantitative cell biology. *Biotechnol. Bioeng.* 2006, *94*, 5–14.

[10] Mosadegh, B., Agarwal, M., Tavana, H., Bersano-Begey, T. *et al.*, Uniform cell seeding and generation of overlapping gradient profiles in a multiplexed microchamber device with normally-closed valves. *Lab Chip* 2010, *10*, 2959–2964.

[11] Prokop, A., Prokop, Z., Schaffer, D., Kozlov, E. *et al*., Nano-LiterBioReactor: Long-term mammalian cell culture at nanofabricated scale. *Biomed. Microdevices* 2004, *6*, 325–339.

[12] Hung, P., Lee, P., Sabounchi, P., Lin, R., Lee, L., Continuous perfusion microfluidic cell culture array for high-throughput cell-based assays. *Biotechnol. Bioeng.* 2005, *89*, 1–8.

[13] Luo, C., Zhu, X., Yu, T., Luo, X. *et al*., A fast cell loading and high throughput microfluidic system for long term cell culture in zero flow environments. *Biotechnol. Bioeng.* 2008, *101*, 190–195.

[14] Nilsson, J., Evander, M., Hammarström, B., Laurell, T., Review of cell and particle trapping in microfluidic systems. *Anal. Chim. Acta* 2009, *649*, 141–157.

[15] Brouzes, E., Medkova, M., Savenelli, N., Marran, D. *et al*., Droplet microfluidic technology for single-cell high-throughput screening. *Proc. Natl. Acad. Sci. USA.* 2009, *106*, 14195–14200.

[16] Clausell-Tormos, J., Lieber, D., Baret, J. C., El-Harrak, A. *et al*., Droplet-based microfluidic platforms for the encapsulation and screening of mammalian cells and multicellular organisms. *Chem. Biol.* 2008, *15*, 427–437.

[17] Wang, Z., Kim, M. C., Marquez, M., Thorsen, T., High-density microfluidic arrays for cell cytotoxicity analysis. *Lab Chip* 2007, *7*, 740–745.

[18] Yang, M., Li, C., Yang, J., Cell docking and on-chip monitoring of cellular reactions with a controlled concentration gradient on a microfluidic device. *Anal. Chem.* 2002, *74*, 3991–4001.

[19] Conant, C. G., Schwartz, M. A., Ionescu-Zanetti, C., Well plate-coupled microfluidic devices designed for facile image-based cell adhesion and transmigration assays. *J. Biomol. Screen*. 2010, *15*, 102–106.

[20] Lau, A. Y., Hung, P. J., Wu, A. R., Lee, L. P., Open-access microfluidic patch-clamp array with raised lateral cell trapping sites. *Lab Chip* 2006, *6*, 1510–1515.

[21] Rosenthal, A., Macdonald, A., Voldman, J., Cell patterning chip for controlling the stem cell microenvironment. *Biomaterials* 2007, *28*, 3208–3216.

[22] Park, M. C., Hur, J. Y., Cho, H. S., Park, S.-H., Suh, K. Y., High-throughput single-cell quantification using simple microwell-based cell docking and programmable time-course live-cell imaging. *Lab Chip* 2011, *11*, 79–86.

[23] Hung, P. J., Lee, P. J., Sabounchi, P., Aghdam, N. *et al*., A novel high aspect ratio microfluidic design to provide a stable and uniform microenvironment for cell growth in a high throughput mammalian cell culture array. *Lab Chip* 2005, *5*, 44–48.

[24] Han, C., Zhang, Q., Ma, R., Xie, L. *et al*., Integration of single oocyte trapping, in vitro fertilization and embryo culture in a microwell-structured microfluidic device. *Lab Chip* 2010, *10*, 2848–2854.

[25] Cioffi, M., Moretti, M., Manbachi, A., Chung, B. *et al*., A computational and experimental study inside microfluidic systems: the role of shear stress and flow recirculation in cell docking. *Biomed. Microdevices* 2010, *12*, 619–626.

[26] Unger, M., Chou, H., Thorsen, T., Scherer, A., Quake, S., Monolithic microfabricated valves and pumps by multilayer soft lithography. *Science* 2000, *288*, 113–116.

[27] Guillou, H., Depraz-Depland, A., Planus, E., Vianay, B. *et al*., Lamellipodia nucleation by filopodia depends on integrin occupancy and downstream Rac1 signaling. *Exp. Cell Res.* 2008, *314*, 478–488.

[28] Manbachi, A., Shrivastava, S., Cioffi, M., Chung, B. *et al*., Microcirculation within grooved substrates regulates cell positioning and cell docking inside microfluidic channels. *Lab Chip* 2008, *8*, 747–754.

[29] Gaver, D., Kute, S., A theoretical model study of the influence of fluid stresses on a cell adhering to a microchannel wall. *Biophys. J.* 1998, *75*, 721–733.

[30] Wu, L., Di Carlo, D., Lee, L., Microfluidic self-assembly of tumor spheroids for anticancer drug discovery. *Biomed. Microdevices* 2008, *10*, 197–202.

[31] Leach, A., Wheeler, A., Zare, R., Flow injection analysis in a microfluidic format. *Anal. Chem.* 2003, *75*, 967–972.

[32] Khabiry, M., Chung, B., Hancock, M., Soundararajan, H. *et al*., Cell docking in double grooves in a microfluidic channel. *Small* 2009, *5*, 1186–1194.

[33] Chang, T. Y., Yadav, V. G., De Leo, S., Mohedas, A. *et al*., Cell and protein compatibility of parylene-C surfaces. *Langmuir* 2007, *23*, 11718–11725.

[34] Leclerc, E., David, B., Griscom, L., Lepioufle, B. *et al*., Study of osteoblastic cells in a microfluidic environment. *Biomaterials* 2006, *27*, 586–595.

[35] Malda, J., Rouwkema, J., Martens, D., Le Comte, E. *et al*., Oxygen gradients in tissue-engineered PEGT/PBT cartilaginous constructs: Measurement and modeling. *Biotechnol. Bioeng.* 2004, *86*, 9–18.

[36] Wu, F., Li, L., Xu, Z., Tan, S., Zhang, Z., Transport study of pure and mixed gases through PDMS membrane. *Chem. Eng. J.* 2006, *117*, 51–59.